

# Downlink Massive MU-MIMO with Successively-Regularized Zero Forcing Precoding

Aravindh Krishnamoorthy<sup>†\*</sup> and Robert Schober<sup>†</sup>

<sup>†</sup>Friedrich-Alexander-Universität Erlangen-Nürnberg, Germany, <sup>\*</sup>Fraunhofer Institute for Integrated Circuits (IIS) Erlangen, Germany

**Abstract**—In this letter, we consider linear precoding for downlink massive multi-user (MU) multiple-input multiple-output (MIMO) systems. We propose the novel successively-regularized zero forcing (SRZF) precoding, which exploits successive null spaces of the MIMO channels of the users, along with regularization, to control the inter-user interference and to enhance performance and robustness to imperfect channel state information (CSI) at the base station (BS). We compare the weighted sum rate of the proposed SRZF precoding with those of block diagonalization and conventional and regularized zero forcing precoding for fixed and locally-optimal power allocation strategies as well as for perfect and imperfect CSI via computer simulations. Our simulation results reveal that for both underloaded and critically-loaded systems and perfect and imperfect CSI at the BS, the proposed SRZF precoding significantly outperforms the considered baseline schemes, making it an attractive option for downlink massive MU-MIMO systems.

## I. INTRODUCTION

Massive multi-user (MU) multiple-input multiple-output (MIMO) is a promising technology for the 6th generation (6G) and beyond communication systems where base stations (BSs) will employ a large number of antennas for transmission and reception [1]. For downlink massive MU-MIMO systems, linear zero forcing (ZF) precoding [2], [3] has been shown to be asymptotically optimal as the number of BS antennas grows large while the number of users is kept constant [1].

However, in practical systems, ZF precoding achieves a high performance only in severely underloaded systems, where the total number of user antennas is much smaller than the number of BS antennas, and when the user channels are sufficiently distinct. On the other hand, for overloaded and critically-loaded systems, where the total number of user antennas is greater than or equal to the number of BS antennas, and when the user channels are correlated, ZF precoding suffers from poor performance, see, e.g., [4]. Alternatively, block diagonalization (BD) [5] has a slightly better performance than ZF precoding in critically-loaded systems. However, BD precoding suffers from poor performance in underloaded systems, see, e.g., simulation results in [4], [6].

In order to overcome the poor performance of ZF precoding and to enhance the robustness to imperfect channel state information (CSI) at the BS, regularized ZF (RZF) precoding was proposed in [7], where regularization constants were utilized to overcome the challenges arising from the inversion of rank deficient matrices. However, RZF precoding introduces

significant inter-user interference (IUI), which limits its performance, see, e.g., [4], [8].

On the other hand, successive null space (SNS) precoding, which exploits successive null spaces of the MIMO channel matrices of the users to enhance the performance and robustness to imperfect CSI at the BS, was proposed recently in [4], in the context of MIMO rate-splitting multiple access (RSMA). SNS precoding can also be utilized as a linear precoding scheme if rate splitting and successive interference cancellation are to be avoided. In [4], SNS precoding was shown to achieve superior performance compared to BD, ZF, and RZF precoding for both perfect and imperfect CSI at the BS. Unfortunately, the algorithm for computing the SNS precoders provided in [4] entails a comparatively high computational complexity, limiting its practical applicability.

In this letter, we develop the novel, low-complexity successively-regularized zero forcing (SRZF) linear precoding scheme, which exploits successive null spaces of the MIMO channels of the users, along with regularization, to control the IUI and enhance performance and robustness to imperfect CSI at the BS. The main contributions of this letter are as follows.

- We present the novel SRZF precoding scheme for fixed and locally-optimal power allocation (PA) strategies.
- We compare the weighted sum rate (WSR) performance of the proposed SRZF precoding with those of SNS [4], BD [5], ZF [2], and RZF [7] precoding via simulations.

Our simulation results reveal that, for both underloaded and critically-loaded systems and for both perfect and imperfect CSI at the BS, the proposed SRZF precoding scheme significantly outperforms conventional BD, ZF, and RZF precoding, and provides a low-complexity alternative to SNS precoding with a moderate loss in performance.

The remainder of this letter is organized as follows. In Section II, we provide the system model and a brief review of SNS precoding [4]. In Section III, we describe the proposed SRZF precoding and decoding schemes. Fixed and locally-optimal PA strategies are investigated in Section IV. Simulation results are presented in Section V, and the letter is concluded in Section VI.

*Notation:* Boldface capital letters  $\mathbf{X}$  and boldface lowercase letters  $x$  denote matrices and vectors, respectively.  $\mathbf{X}^H$ ,  $\mathbf{X}^+$ , and  $\text{tr}(\mathbf{X})$  denote the Hermitian transpose, pseudo-inverse, and trace of matrix  $\mathbf{X}$ , respectively.  $\mathbb{C}^{m \times n}$  and  $\mathbb{R}^{m \times n}$  denote the sets of  $m \times n$  matrices with complex-valued and real-valued entries, respectively. The  $(i, j)$ -th entry of matrix  $\mathbf{X}$  is denoted by  $[\mathbf{X}]_{i,j}$  and the  $i$ -th element of vector  $x$  is denoted by  $[x]_i$ .  $\mathbf{I}_n$  denotes the  $n \times n$  identity matrix. The circularly

The authors acknowledge the financial support by the Federal Ministry of Education and Research of Germany in the programme of “Souverän. Digital. Vernetzt.” joint project 6G-RIC, project identification number: PIN 16KISK023.

symmetric complex-valued Gaussian distribution with mean  $\boldsymbol{\mu}$  and covariance matrix  $\boldsymbol{\Sigma}$  is denoted by  $\mathcal{CN}(\boldsymbol{\mu}, \boldsymbol{\Sigma})$ ;  $\sim$  stands for “distributed as”.  $\mathbb{E}[\cdot]$  denotes statistical expectation.  $\mathcal{D}[\mathbf{X}]$  denotes the diagonal matrix formed by setting all the off-diagonal elements of  $\mathbf{X}$  to zero.

## II. PRELIMINARIES

In this section, we present the considered downlink MIMO system model, the imperfect CSI model, and a brief review of SNS precoding [4].

### A. System Model

We consider an *underloaded* or *critically loaded* downlink MU-MIMO communication system comprising a BS with  $N$  transmit antennas and  $K$  users equipped with  $M_k, k = 1, \dots, K$ , antennas such that  $N \geq \sum_{k=1}^K M_k = M$ , where  $M$  denotes the total number of user antennas.

We assume that  $M_k$  streams are transmitted to user  $k, k = 1, \dots, K$ . If fewer streams are desired, then, user  $k$ 's MIMO channel can be transformed into a matrix with fewer effective receive antennas via singular value decomposition (SVD) [3] and  $M_k$  can be redefined accordingly. Let  $\mathbf{s}_k \in \mathbb{C}^{M_k \times 1}$  denote the MIMO symbol vector of user  $k$  satisfying  $\mathbb{E}[\mathbf{s}_k \mathbf{s}_k^H] = \mathbf{I}_{M_k}, k = 1, \dots, K$ . We assume that the  $[\mathbf{s}_k]_i, i = 1, \dots, M_k, k = 1, \dots, K$ , are independent. For transmission,  $\mathbf{s}_k$  is precoded using linear precoder  $\mathbf{P}_k \in \mathbb{C}^{N \times M_k}, k = 1, \dots, K$ , to obtain overall transmit signal  $\mathbf{x} = \sum_{k=1}^K \mathbf{P}_k \mathbf{s}_k$ . The power constraint at the BS is given by

$$\sum_{k=1}^K \text{tr}(\mathbf{P}_k \mathbf{P}_k^H) \leq P_T, \quad (1)$$

where  $P_T$  denotes the available transmit power. Let  $\frac{1}{\sqrt{L_k}} \mathbf{H}_k \in \mathbb{C}^{M_k \times N}$  denote the MIMO channel matrix between the BS and user  $k$ , where scalar  $L_k$  models the path loss between the BS and user  $k$ , and  $\mathbf{H}_k$  models the small scale fading. Here, we assume that all MIMO channel matrices have full row rank<sup>1</sup>. Then, the received signal at user  $k$  is given by

$$\mathbf{y}_k = \frac{1}{\sqrt{L_k}} \mathbf{H}_k \mathbf{x} + \mathbf{z}_k = \frac{1}{\sqrt{L_k}} \mathbf{H}_k \sum_{k'=1}^K \mathbf{P}_{k'} \mathbf{s}_{k'} + \mathbf{z}_k, \quad (2)$$

where  $\mathbf{z}_k \in \mathbb{C}^{M_k \times 1} \sim \mathcal{CN}(\mathbf{0}, \sigma^2 \mathbf{I}_{M_k})$  denotes the complex additive white Gaussian noise (AWGN) vector at user  $k$ .

### B. Imperfect CSI Model

In this letter, we assume that only quantized and outdated MIMO channel matrices  $\bar{\mathbf{H}}_k, k = 1, \dots, K$ , are available at the BS for computing the precoders. Nevertheless, we assume that the BS knows<sup>2</sup> scalar  $L_k$  perfectly, and the users know

<sup>1</sup>We note that a row-rank deficient MIMO channel matrix can be transformed into a full row-rank matrix with fewer effective receive antennas via SVD, see, e.g., [3], [9, App. C].

<sup>2</sup>This assumption is motivated by the slow variation of path loss  $L_k$  and the resulting low feedback requirement.

their own MIMO channel matrices perfectly<sup>3</sup>. We model the imperfect MIMO channel matrices at the BS as  $\frac{1}{\sqrt{L_k}} \bar{\mathbf{H}}_k = \frac{1}{\sqrt{L_k}} \mathbf{H}_k + \frac{1}{\sqrt{L_k}} \Delta \mathbf{H}_k, k = 1, \dots, K$ , where  $L_k$  and  $\mathbf{H}_k$  denote the actual path loss coefficient and the MIMO channel matrix of user  $k$ , respectively, and  $\Delta \mathbf{H}_k \in \mathbb{C}^{M_k \times N}$  models the CSI error at the BS [10].

### C. SNS Precoding

Let  $\boldsymbol{\Psi}_k \in \mathbb{C}^{N \times N_k}, N_k = N - \sum_{k'=1}^{k-1} M_{k'}$ , denote a matrix whose columns are the unit-length basis vectors of the null space of the following augmented matrix:

$$\mathbf{F}_k = [\mathbf{H}_1^T \quad \mathbf{H}_2^T \quad \dots \quad \mathbf{H}_{k-1}^T]^T \in \mathbb{C}^{(N-N_k) \times N}, \quad (3)$$

with the convention  $\boldsymbol{\Psi}_1 = \mathbf{I}_N$ . The SNS precoder [4] for user  $k$  is constructed as  $\mathbf{P}_k = \boldsymbol{\Psi}_k \mathbf{W}_k^{\frac{1}{2}}$ , where  $\mathbf{W}_k \in \mathbb{C}^{N_k \times M_k}$  is a rectangular matrix, which is used for combining the column vectors of  $\boldsymbol{\Psi}_k$  into the precoding vectors and for PA. Furthermore, for SNS precoding, the power constraint in (1) can be rewritten as  $\sum_{k=1}^K \text{tr}(\mathbf{W}_k \mathbf{W}_k^H) \leq P_T$ . Now, with SNS precoding, the received signal in (2) simplifies to:

$$\mathbf{y}_k = \frac{1}{\sqrt{L_k}} \mathbf{H}_k \sum_{k'=1}^k \mathbf{P}_{k'} \mathbf{s}_{k'} + \mathbf{z}_k. \quad (4)$$

That is, user  $k$  experiences IUI from users  $1, \dots, k-1$ , and causes IUI to users  $k+1, \dots, K$ , which, for the optimal  $\mathbf{W}_k, k = 1, \dots, K$ , enhances performance and robustness compared to BD, ZF, and RZF precoding, see [4] for details. However, obtaining the optimal  $\mathbf{W}_k, k = 1, \dots, K$ , via [4, Algorithm 1] is computationally complex, limiting the applicability of SNS precoding in practice.

## III. PROPOSED SRZF PRECODING AND DECODING SCHEMES

In this section, we introduce the proposed SRZF precoding and decoding schemes and determine the resulting achievable user rates.

### A. Precoding Scheme

Let  $\bar{\mathbf{H}} = [\bar{\mathbf{H}}_1^T \quad \dots \quad \bar{\mathbf{H}}_K^T]^T \in \mathbb{C}^{M \times N}$ . Furthermore, let  $m_k = \sum_{k'=1}^{k-1} M_{k'} + 1$  denote the index of the first row of user  $k$ 's channel in  $\bar{\mathbf{H}}$ , defined above. Moreover, let  $\mathbf{J}_k \in \mathbb{R}^{M \times M}$  denote a real-valued, diagonal matrix such that  $[\mathbf{J}_k]_{i_k, i_k} = 1, i_k = m_{k+1}, \dots, M, k = 1, \dots, K-1$ , and the remaining elements are zeros, with the convention  $\mathbf{J}_K = \mathbf{0}$ . Then, the precoder matrix for user  $k, \mathbf{P}_k \in \mathbb{C}^{N \times M_k}$ , is chosen as:

$$\mathbf{P}_k = \bar{\mathbf{H}}^H \boldsymbol{\Phi}_k \mathbf{D}_k^{\frac{1}{2}}, \quad (5)$$

where  $\boldsymbol{\Phi}_k = [\phi_{k,1}, \dots, \phi_{k,M_k}] \in \mathbb{C}^{N \times M_k}$  contains columns  $m_k, \dots, m_k + M_k - 1$  of matrix  $(\bar{\mathbf{H}} \bar{\mathbf{H}}^H + \alpha_k \mathbf{J}_k)^{-1}, \alpha_k > 0, k = 1, \dots, K$ , is a small regularization constant whose role is described later, and  $\mathbf{D}_k \in \mathbb{R}^{M_k \times M_k} \succcurlyeq \mathbf{0}, k = 1, \dots, K$ , is

<sup>3</sup>In practice, the MIMO channels matrices can be estimated frequently and accurately at the receivers by exploiting, e.g., high-power pilot sequences transmitted by the BS.

the diagonal power-allocation matrix, which based on (1) and (5) has to satisfy the power constraint:

$$\sum_{k=1}^K \text{tr} \left( \bar{\mathbf{H}}^H \Phi_k \mathbf{D}_k \Phi_k^H \bar{\mathbf{H}} \right) \leq P_T. \quad (6)$$

*Remark 1.* SRZF precoding reduces to ZF precoding for  $\alpha_k = 0, k = 1, \dots, K$ , and to RZF precoding if  $\alpha_k \mathbf{J}_k$  is replaced by  $\alpha_k \mathbf{I}_M, k = 1, \dots, K$ . A more general version of SRZF precoding can also be obtained by utilizing an arbitrary (diagonal) regularization matrix instead of  $\alpha_k \mathbf{J}_k$ .

Next, in the following proposition, we show that the precoder in (5) is a special case of SNS precoding [4].

**Proposition 1.** *For perfect CSI, i.e.,  $\Delta \mathbf{H}_k = \mathbf{0}, k = 1, \dots, K$ , we have:*

$$\mathbf{H}_k \mathbf{P}_{k'} = \begin{cases} -\alpha_{k'} \bar{\Phi}_{k'} \mathbf{D}_{k'}^{\frac{1}{2}} & \text{if } k' < k \\ \mathbf{D}_k^{\frac{1}{2}} & \text{if } k' = k \\ \mathbf{0} & \text{if } k' > k, \end{cases} \quad (7)$$

where  $\bar{\Phi}_{k'} \in \mathbb{C}^{M_k \times M_{k'}}$  contains rows  $m_k, \dots, m_k + M_k - 1$  of  $\Phi_{k'}$ .

*Proof.* Please see Appendix A.  $\square$

Based on (2) and Proposition 1, the received signal at user  $k$  can be simplified to

$$\mathbf{y}_k = \mathbf{D}_k^{\frac{1}{2}} \mathbf{s}_k - \sum_{k'=1}^{k-1} \alpha_{k'} \bar{\Phi}_{k'} \mathbf{D}_{k'}^{\frac{1}{2}} \mathbf{s}_{k'} + \mathbf{z}_k. \quad (8)$$

As seen from (8), SRZF precoding is a special case of SNS precoding [4], described earlier in Section II-C. That is, for SRZF precoding, user  $k$  experiences IUI from users  $1, \dots, k-1$ , and causes IUI to users  $k+1, \dots, K$ . Furthermore, the IUI for user  $k$  caused by users  $1, \dots, k-1$  can be adjusted using the regularization constants  $\alpha_k, k = 1, \dots, K$ . In this letter, based on [7], we set  $\alpha_1 = \dots = \alpha_K = \frac{M\sigma^2}{P_T}$ . Nevertheless, we note that the performance of the proposed SRZF precoders may be further enhanced by optimizing the values of  $\alpha_k, k = 1, \dots, K$ , for a given deployment scenario.

*Remark 2.* As seen from Proposition 1, the IUI experienced by a user depends on the user index, i.e., user 1 experiences no IUI and user  $K$  experiences IUI from all other users. Hence, SNS precoding is sensitive to user ordering [4]. In this letter, we utilize the suboptimal fixed user-index permutation described in [4]. Nevertheless, the performance of SRZF precoding can also be further improved by determining the optimal user ordering via an exhaustive search.

### B. Decoding at the Receivers

Substituting (5) into (2), the received signal at user  $k$  can be simplified to:

$$\mathbf{y}_k = \frac{1}{\sqrt{L_k}} \mathbf{G}_{k,k} \mathbf{D}_k^{\frac{1}{2}} \mathbf{s}_k + \mathbf{u}_k + \mathbf{z}_k, \quad (9)$$

where  $\mathbf{G}_{k,k'} = \mathbf{H}_k \bar{\mathbf{H}}^H \Phi_{k'} \in \mathbb{C}^{M_k \times M_{k'}}, k = 1, \dots, K$ , is the effective MIMO channel of user  $k$  for the symbol vector of user  $k'$  and  $\mathbf{u}_k = \frac{1}{\sqrt{L_k}} \sum_{k'=1, k' \neq k}^K \mathbf{G}_{k,k'} \mathbf{D}_{k'}^{\frac{1}{2}} \mathbf{s}_{k'} \in \mathbb{C}^{M_k \times 1}$  is the IUI for user  $k$ . Here, at user  $k$ , based on (9), the elements of  $\mathbf{s}_k$  are decoded jointly treating  $\mathbf{u}_k$  as noise.

### C. Achievable Rates

Based on (9), the achievable rate for the symbol vector of user  $k, k = 1, \dots, K$ , is given as follows:

$$R_k = \log_2 \det \left( \mathbf{I}_{M_k} + \frac{1}{L_k} \mathbf{G}_{k,k} \mathbf{D}_k \mathbf{G}_{k,k}^H \mathbf{N}_k^{-1} \right), \quad (10)$$

where  $\mathbf{N}_k = \sigma^2 \mathbf{I}_{M_k} + \frac{1}{L_k} \sum_{k'=1, k' \neq k}^K \mathbf{G}_{k,k'} \mathbf{D}_{k'} \mathbf{G}_{k,k'}^H$ .

## IV. POWER ALLOCATION

In this section, we describe fixed and locally-optimal PA schemes for obtaining  $\mathbf{D}_k, k = 1, \dots, K$ .

### A. Fixed Power Allocation

For fixed power allocation (FPA), we choose

$$[\mathbf{D}_k]_{l,l} = \frac{P_T}{M \text{tr} \left( \phi_{k,l} \phi_{k,l}^H \right)}, \quad (11)$$

for  $k = 1, \dots, K, l = 1, \dots, M_k$ , which satisfies (6). Here,  $\phi_{k,l}$  is the  $l$ -th column of  $\Phi_k$ , as defined in Section III-A.

While FPA has good performance when the user channels are uncorrelated, for highly correlated user channels, optimal PA yields substantial gains. Hence, in the following, we utilize WSR maximization as the criterion for obtaining the optimal PA.

### B. Weighted Sum Rate Maximization

The WSR is given by  $R_{\text{WSR}} = \sum_{k=1}^K \eta_k R_k$ , where  $0 \leq \eta_k \leq 1, k = 1, \dots, K, \sum_{k=1}^K \eta_k = 1$ , denote fixed weights which can be chosen to adjust the rates of the users during PA [11, Sec. 4].

We note that the WSR depends on the actual channel  $\mathbf{H}$ . However, for WSR maximization at the BS, only  $\bar{\mathbf{H}}$  is available. Hence, we define  $\bar{\mathbf{G}}_{k,k'} = \bar{\mathbf{H}}_k \bar{\mathbf{H}}^H \Phi_{k'} \in \mathbb{C}^{M_k \times M_{k'}}, k = 1, \dots, K$ , and obtain  $\bar{R}_k, k = 1, \dots, K$ , and  $\bar{R}_{\text{WSR}}$ , analogously to (10) and  $R_{\text{WSR}}$ , respectively, where  $\mathbf{G}_{k,k'}$  is replaced by  $\bar{\mathbf{G}}_{k,k'}, k, k' = 1, \dots, K$ . Then,  $\bar{R}_{\text{WSR}}$ , which only depends on the imperfect CSI available at the BS, is used as the objective for WSR maximization.

Next, the WSR maximization problem at the BS can be formulated as follows.

$$\bar{R}_{\text{WSR}}^* = \underset{\substack{\mathbf{D}_k \text{ diagonal} \\ \mathbf{D}_k \succ \mathbf{0}, k=1, \dots, K}}{\text{maximize}} \bar{R}_{\text{WSR}} \quad \text{subject to (6)}. \quad (12)$$

Solving (12) optimally entails a high computational complexity due to the non-convex objective function. Hence, in the following, we provide a locally optimal solution obtained via iterative SCA [12], see [4, Algorithm 1] for a similar algorithm.

### C. Successive Convex Approximation

In iteration  $l = 1, 2, \dots$ , a convex approximation of the objective function  $\tilde{R}_{\text{WSR}}$ , denoted by  $\tilde{R}_{\text{WSR}}$ , is constructed based on a first-order approximation around *given points*  $\mathbf{D}_k^{(l-1)} \in \mathbb{C}^{M_k \times M_k}, k = 1, \dots, K$ , with initial values  $\mathbf{D}_k^{(0)} = \mathbf{0}, k = 1, \dots, K$ , as  $\tilde{R}_{\text{WSR}} = \sum_{k=1}^K \eta_k \tilde{R}_k$ , where  $\tilde{R}_k$  is given in (??) on top of the next page and  $\Xi_k = \mathbf{I}_{M_k} + \frac{1}{L_k} \sum_{k'=1, k' \neq k}^K \tilde{\mathbf{G}}_{k,k'} \mathbf{D}_{k'}^{(l-1)} \tilde{\mathbf{G}}_{k,k'}^H$ , see [4, Lemma 1] for details. Next, an inner convex optimization problem with  $\tilde{R}_{\text{WSR}}$  as the objective function is constructed as follows:

$$\tilde{R}_{\text{WSR}}^* = \underset{\substack{\mathbf{D}_k \text{ diagonal} \\ \mathbf{D}_k \succ \mathbf{0}, k=1, \dots, K}}{\text{maximize}} \tilde{R}_{\text{WSR}} \quad \text{subject to (6)}. \quad (13)$$

The inner convex optimization problem (13) is solved using standard convex optimization tools [13] to obtain the optimal value,  $\tilde{R}_{\text{WSR}}^{*(l)}$ , and the corresponding optimal solution  $\mathbf{D}_k^*, k = 1, \dots, K$ . The obtained solution is used for computing the first-order approximation for the next iteration. This process gradually tightens the first-order approximation of the objective function around a local optimum of (12). Hence, the corresponding sequence of optimal values of (13),  $\tilde{R}_{\text{WSR}}^{*(l)}, l = 1, 2, \dots$ , converges to a local optimum of (12) [12]. The iterations are continued until convergence, up to a numerical tolerance  $\epsilon$  or for  $N_{\text{iter}}$  iterations.

### D. Computational Complexity

For the proposed SRZF scheme with FPA, computing  $\Phi_K$  in (5) via Cholesky decomposition and equation solving entails a total complexity of  $\mathcal{O}(MN^2 + \frac{1}{6}M^3 + \frac{1}{3}M_K M^2)$  [14]. Next, computing  $\Phi_k, k = 1, \dots, K-1$ , entails a complexity of  $\mathcal{O}(MN^2 + \frac{1}{2}M^2 + \frac{1}{3}(M - M_K)M^2)$ . Hence, SRZF precoding entails an overall complexity of  $\mathcal{O}(2MN^2 + \frac{1}{2}M^3 + \frac{1}{2}M^2)$ , which is only marginally higher than the complexity for RZF and ZF precoding, given by  $\mathcal{O}(2MN^2 + \frac{1}{2}M^3)$ , and BD precoding, given by  $\mathcal{O}(2MN^2 + \sum_{k=1}^K M_k^3)$ , see [4] for details.

For the locally-optimal PA via SCA [12], the proposed SRZF and RZF precoding schemes entail an additional complexity of  $\mathcal{O}(N_{\text{iter}} M \sqrt{M} \log(1/\epsilon))$  [12], where  $N_{\text{iter}}$  is the number of SCA iterations. However, the PA for BD and ZF precoding entails a lower complexity of  $\mathcal{O}(M \sqrt{M} \log(1/\epsilon))$  because the corresponding WSR maximization problems are convex, see [4] for details.

On the other hand, computing the precoding vectors and PA for SNS precoding in Section II-C via [4, Algorithm 1] entails a significantly higher computational complexity of  $\mathcal{O}(2MN^2 + N_{\text{iter}} (\sum_{k=1}^K N_k^2)^{\frac{3}{2}} \log(1/\epsilon))$ .

## V. SIMULATION RESULTS

In this section, we compare the WSR of the proposed SRZF precoding with the WSRs of SNS [4], conventional BD [5], ZF [2], and RZF [7] precoding for perfect and imperfect CSI via computer simulations. We assume that all schemes employ

joint decoding at the receivers. For RZF precoding, based on [7], we set the regularization constant to  $\frac{M\sigma^2}{P_T}$ .

In Figures 1 and 2, we consider *critically-loaded* and *underloaded* systems, respectively, with  $K = 64$  and  $K = 32$  users, respectively,  $N = 128$  BS antennas, and  $M_k = 2$  antennas per user. The  $K$  users are located equidistantly from the BS at distances of  $d_k = 50$  m,  $k = 1, \dots, K$ . The scalar path loss for user  $k, L_k$ , is set to  $d_k^2$ . Furthermore, the user weights are set to be equal, i.e.,  $\eta_k = \frac{1}{K}$ . Moreover, for imperfect CSI, the additive i.i.d. Gaussian error model, where the elements of  $\Delta \mathbf{H}_k, k = 1, \dots, K$ , have zero mean and variance  $\mu_k$ , is adopted.

In Figure 1, i.i.d. Gaussian user MIMO channel matrices, whose elements have zero mean and unit variance, are assumed. The noise variance is set to  $\sigma^2 = -35$  dBm, and for imperfect CSI,  $\mu_k = 0.1, k = 1, \dots, K$ . For obtaining the WSR curves, we utilize FPA for the proposed and the baseline schemes, except for SNS precoding, for which we utilize the baseline SCA-based scheme given in [4].

On the other hand, for Figure 2, we adopt the QuaDRiGa channel model [15] employing the 3GPP\_38.901\_UMa scenario. Furthermore, we set the user locations as follows. Users  $1, \dots, \frac{K}{2}$  are spread uniformly around the BS and experience distinct MIMO channels. However, users  $\frac{K}{2} + 1, \dots, K$ , are located within an angular spread of  $0.5^\circ$  from users  $1, \dots, \frac{K}{2}$ , respectively. This causes a high correlation in the MIMO channels experienced by users  $k$  and  $\frac{K}{2} + k, k = 1, \dots, \frac{K}{2}$ . The noise variance is set to  $\sigma^2 = -90$  dBm, and for imperfect CSI, we set  $\mu_k = 0.01$ . Furthermore, we utilize SCA-based PA for the proposed and the baseline schemes.

From Figures 1 and 2, we observe that the proposed SRZF precoding scheme significantly outperforms BD, ZF, and RZF precoding for both perfect and imperfect CSI by exploiting successive null spaces and regularization, thereby providing an attractive alternative to these conventional schemes for deployment in massive MU-MIMO systems. The SNS precoding from [4], which utilizes high-complexity SCA-based precoding vector selection and PA [4], achieves a moderate WSR increase of 2–2.5 bits per channel use (BPCU) over the proposed SRZF precoding scheme, which entails a substantially lower computational complexity.

## VI. CONCLUSION

In this letter, we considered linear precoding for downlink massive MU-MIMO systems. We proposed the novel SRZF precoding scheme, which exploits successive null spaces of the MIMO channels of the users, along with regularization, to enhance performance and robustness. We showed in Proposition 1 that SRZF precoding is a special case of SNS precoding [4], thereby inheriting its good performance and robustness to imperfect CSI. We discussed fixed and locally-optimal PA strategies and utilized them to compare the performance of the proposed scheme with those of SNS, BD, ZF, and RZF precoding via computer simulations. Our results showed that for underloaded and critically-loaded systems and perfect and imperfect CSI at the BS, the proposed SRZF precoding

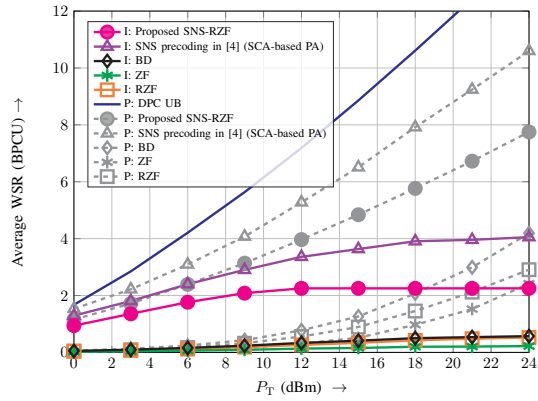


**Fig. 1:** Average WSR as a function of  $P_T$  for a critically-loaded system for equidistant users,  $K = 64$ ,  $N = 128$ ,  $M_k = 2$ ,  $d_k = 50$  m,  $\eta_k = \frac{1}{K}$ ,  $\mu_k = 0.1$ , for  $k = 1, \dots, K$ ,  $\sigma^2 = -35$  dBm, the i.i.d. Gaussian MIMO channel model, and FPA<sup>4</sup>. P: Perfect CSI, I: Imperfect CSI.

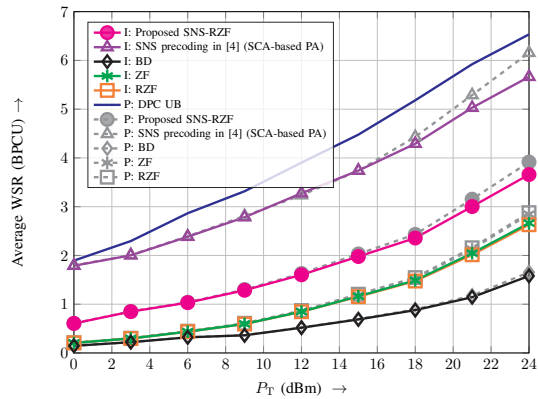


**Fig. 2:** Average WSR as a function of  $P_T$  for an underloaded (50% load) system for paired users,  $K = 32$ ,  $N = 128$ ,  $M_k = 2$ ,  $d_k = 50$  m,  $\eta_k = \frac{1}{K}$ ,  $\mu_k = 0.01$ , for  $k = 1, \dots, K$ ,  $\sigma^2 = -90$  dBm, the QuaDRiGa channel model [15], and SCA-based PA. P: Perfect CSI, I: Imperfect CSI.

outperforms the conventional schemes and provides a low-complexity alternative to SNS precoding with moderate loss in performance, making it an attractive option for downlink massive MU-MIMO systems.

The optimization of the regularization factors and user index permutations, taking into account the deployment scenario and CSI quality of the users, are interesting topics for future study for further enhancing the performance and robustness of SRZF precoding.

#### APPENDIX A: PROOF OF PROPOSITION 1

We note that, as  $\Delta \mathbf{H}_k = \mathbf{0}$ ,  $k = 1, \dots, K$ , we have  $\bar{\mathbf{H}} = \mathbf{H}$ . Next, since  $(\mathbf{H}\mathbf{H}^H + \alpha_{k'}\mathbf{J}_{k'})^{-1}(\mathbf{H}\mathbf{H}^H + \alpha_{k'}\mathbf{J}_{k'})^{-1} = \mathbf{I}_M$ ,

<sup>4</sup>The curves for SNS precoding in [4] utilize SCA for determining the precoding vectors and for PA.

$k' = 1, \dots, K$ , we have

$$\begin{aligned} & \mathbf{H}\mathbf{H}^H(\mathbf{H}\mathbf{H}^H + \alpha_{k'}\mathbf{J}_{k'})^{-1} \\ &= \mathbf{I}_M - \alpha_{k'}\mathbf{J}_{k'}(\mathbf{H}\mathbf{H}^H + \alpha_{k'}\mathbf{J}_{k'})^{-1}. \end{aligned} \quad (15)$$

Now, selecting the columns  $m_{k'}, \dots, m_{k'} + M_{k'} - 1$  of the matrices on the left and right hand side of (15), we obtain:

$$\mathbf{H}\mathbf{H}^H\Phi_{k'} = \begin{bmatrix} \mathbf{0}_{\sum_{k''=1}^{k'-1} M_{k''} \times M_{k'}} \\ \mathbf{I}_{M_{k'}} \\ \mathbf{0} \end{bmatrix} - \alpha_{k'}\mathbf{J}_{k'}\Phi_{k'}. \quad (16)$$

Next, selecting rows  $m_k, \dots, m_k + M_k - 1$  of the matrices on the left and right hand side of (16), noting that the first  $\sum_{k''=1}^{k'-1} M_{k''}$  rows of  $\mathbf{J}_{k'}\Phi_{k'}$  are zeros, and utilizing the definition of  $\mathbf{P}_k$  in (5), we obtain (7).  $\square$

#### REFERENCES

- [1] E. G. Larsson, O. Edfors, F. Tufvesson, and T. L. Marzetta, "Massive MIMO for next generation wireless systems," *IEEE Commun. Mag.*, vol. 52, pp. 186–195, Feb. 2014.
- [2] A. Wiesel, Y. C. Eldar, and S. Shamai, "Zero-forcing precoding and generalized inverses," *IEEE Trans. Signal Processing*, vol. 56, pp. 4409–4418, Aug. 2008.
- [3] L. Sun and M. R. McKay, "Eigen-based transceivers for the MIMO broadcast channel with semi-orthogonal user selection," *IEEE Trans. Signal Process.*, vol. 58, pp. 5246–5261, Oct. 2010.
- [4] A. Krishnamoorthy and R. Schober, "Downlink MIMO-RSMA with successive null-space precoding," *IEEE Trans. Wireless Commun. (Early Access)*, May 2022. [Online]. Available: <https://doi.org/10.1109/TWC.2022.3173463>
- [5] Q. H. Spencer, A. L. Swindlehurst, and M. Haardt, "Zero-forcing methods for downlink spatial multiplexing in multiuser MIMO channels," *IEEE Trans. Signal Process.*, vol. 52, pp. 461–471, Feb. 2004.
- [6] A. Krishnamoorthy and R. Schober, "Uplink and downlink MIMO-NOMA with simultaneous triangularization," *IEEE Trans. Wireless Commun.*, vol. 20, pp. 3381–3396, Jan. 2021.
- [7] C. Peel, B. Hochwald, and A. Swindlehurst, "A vector-perturbation technique for near-capacity multiantenna multiuser communication-part I: Channel inversion and regularization," *IEEE Trans. Commun.*, vol. 53, pp. 195–202, Feb. 2005.
- [8] H. Sung, S.-R. Lee, and I. Lee, "Generalized channel inversion methods for multiuser MIMO systems," *IEEE Trans. Commun.*, vol. 57, pp. 3489–3499, Nov. 2009.
- [9] G. Scutari, D. P. Palomar, and S. Barbarossa, "The MIMO iterative waterfilling algorithm," *IEEE Tran. Sig. Proc.*, vol. 57, pp. 1917–1935, Jan. 2009.
- [10] C. Wang, E. K. Au, R. D. Murch, W. H. Mow, R. S. Cheng, and V. Lau, "On the performance of the MIMO zero-forcing receiver in the presence of channel estimation error," *IEEE Trans. Wireless Commun.*, vol. 6, pp. 805–810, Mar. 2007.
- [11] X. Wang and G. B. Giannakis, "Resource allocation for wireless multiuser OFDM networks," *IEEE Trans. Inf. Theory*, vol. 57, pp. 4359–4372, Jun. 2011.
- [12] M. Razaviyayn, "Successive convex approximation: Analysis and applications," Ph.D. dissertation, Univ. of Minnesota, May 2014.
- [13] S. Boyd and L. Vandenberghe, *Convex Optimization*. Cambridge University Press, 2004.
- [14] A. Krishnamoorthy and D. Menon, "Matrix inversion using Cholesky decomposition," in *IEEE Signal Proc.: Algorithms, Architectures, Arrangements, and Applications (SPA) Conf.*, Sep. 2013, pp. 70–72.
- [15] S. Jaeckel, L. Raschkowski, K. Börner, and L. Thiele, "QuaDRiGa: A 3-D multi-cell channel model with time evolution for enabling virtual field trials," *IEEE Trans. Antennas Propagat.*, vol. 62, pp. 3242–3256, Mar. 2014.

# Successively-Regularized Zero Forcing (MATLAB)

Gaussian i.i.d. Channel for a critically-loaded system with  $N=8$ ,  $M_k=2$ ,  $K = 4$  ( $M = K \cdot M_k = 8$ ).

```
K = 4 ;  
MK = 2*ones(K,1) ;  
M = sum(MK) ;  
N = 8 ;  
H = complex(randn(N,M),randn(N,M))/sqrt(2) ;
```

Noise variance is set to unity and the total power is set to 1 W.

```
N0 = 1 ;  
PT = 1 ;
```

Compute the precoder.

```
P = srzf(H,MK,PT,N0) ;
```

Check the precoder to ensure that the SNS design is met, i.e., the combined channel matrix is lower triangular.

```
disp(H*P)
```

Columns 1 through 6

```
1.0000 - 0.0000i  -0.0000 + 0.0000i   0.0000 + 0.0000i  -0.0000 + 0.0000i   0.0000 - 0.0000i   0.0000 - 0.0000i  
-0.0000 + 0.0000i  1.0000 + 0.0000i  -0.0000 + 0.0000i  -0.0000 + 0.0000i   0.0000 - 0.0000i   0.0000 - 0.0000i  
0.0595 + 0.1265i  -0.0479 - 0.2590i   1.0000 - 0.0000i  -0.0000 - 0.0000i  -0.0000 - 0.0000i  -0.0000 - 0.0000i  
0.0178 - 0.1369i   0.1910 - 0.0080i  -0.0000 + 0.0000i   1.0000 + 0.0000i   0.0000 + 0.0000i  -0.0000 - 0.0000i  
0.1678 + 0.0959i  -0.2963 - 0.2226i  -0.0332 + 0.0598i   0.2251 - 0.1220i   1.0000 - 0.0000i   0.0000 + 0.0000i  
0.1401 + 0.1190i  -0.2457 + 0.0503i  -0.1101 + 0.0989i  -0.0093 - 0.0773i  -0.0000 + 0.0000i   1.0000 + 0.0000i  
0.0001 - 0.1496i   0.1024 + 0.1345i   0.1295 + 0.0447i   0.0569 + 0.1259i  -0.3656 + 0.3389i  -0.2848 + 0.1096i  
-0.0898 - 0.2202i   0.3194 + 0.0589i  -0.0148 - 0.3366i   0.0289 - 0.3680i  -0.2102 + 0.4899i   0.0713 + 0.2396i
```

Columns 7 through 8

```
-0.0000 - 0.0000i   0.0000 - 0.0000i  
0.0000 + 0.0000i  -0.0000 + 0.0000i  
-0.0000 + 0.0000i  -0.0000 + 0.0000i  
-0.0000 - 0.0000i  -0.0000 - 0.0000i  
0.0000 + 0.0000i   0.0000 + 0.0000i  
-0.0000 + 0.0000i  -0.0000 - 0.0000i  
1.0000 - 0.0000i  -0.0000 - 0.0000i  
0.0000 + 0.0000i   1.0000 - 0.0000i
```

Function for computing the SRZF precoder.

```
function P = srzf(H,MK,PT,N0)  
K = length(MK) ;  
C = H*H' ;  
P = zeros(size(H')) ;  
for k = K:-1:1  
    CI = inv(C) ;  
    P(:,sum(MK(1:k-1))+1:sum(MK(1:k))) = H'*CI(:,sum(MK(1:k-1))+1:sum(MK(1:k))) ;  
    for l1=sum(MK(1:k-1))+1:sum(MK(1:k))
```

```
    C(11,11) = C(11,11) + sum(MK)*N0/PT ;  
end  
end  
end
```